

Ground state and phase transitions in a system of arg-cysteamines self-assembled on a Au(111) crystal surface

Cite as: J. Chem. Phys. **120**, 954 (2004); <https://doi.org/10.1063/1.1631920>

Submitted: 21 March 2003 . Accepted: 15 October 2003 . Published Online: 31 December 2003

Almas F. Sadreev, Yurii V. Sukhunin, Rodrigo M. Petoral, and Kajsa Uvdal



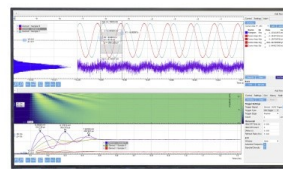
View Online



Export Citation

Challenge us.

What are your needs for
periodic signal detection?



Zurich
Instruments



Ground state and phase transitions in a system of arg-cysteamines self-assembled on a Au(111) crystal surface

Almas F. Sadreev^{a)}

Kirensky Institute of Physics, 660036, Krasnoyarsk, Russia and Department of Physics and Measurement Technology, Linköping University, S-581 83 Linköping, Sweden

Yurii V. Sukhunin

Kirensky Institute of Physics, 660036, Krasnoyarsk, Russia

Rodrigo M. Petoral and Kajsa Uvdal

Department of Physics and Measurement Technology, Linköping University, S-581 83 Linköping, Sweden

(Received 21 March 2003; accepted 15 October 2003)

The translational and orientation order of arg-cysteamine molecules chemisorbed on the Au(111) crystal surface is considered. Couplings between carbon, nitrogen, and hydrogen atoms of the *n*-alkanethiols are approximated by the Lennard-Jones potential. Moreover, hydrogen bonds between oxygen and nitrogen and dipole–dipole interactions of the dipole moments of different atomic groups are taken into account. It is found that molecules are arranged in a 2×2 lattice and have the total symmetry $C_6 \times Z_2$. The critical temperature of the phase transition to the tilted state T_{c1} , which breaks the symmetry C_6 , is estimated to be extremely high. The spontaneous breakdown of the remaining symmetry Z_2 leads to the twisted state of the molecules and has the critical temperature $T_{c2} = 340$ K. © 2004 American Institute of Physics.

[DOI: 10.1063/1.1631920]

I. INTRODUCTION

The self-assembled monolayers (SAMs) are a comparatively new type of organic monolayer,^{1–3} formed by spontaneous chemisorption of long-chain molecules from a solution to many different solid substrates (e.g., Au, Ag, Cu, Al, GaAs, Si). The most thoroughly studied and robust SAM system is $\text{CH}_3(\text{CH}_2)_{n-1}\text{SH}(C_n)$ absorbed on a Au(111) crystal surface. SAMs are presently the focus of considerable attention for both technological and fundamental reasons. Not only do they have potential applications in areas such as corrosion prevention, wear protection, sensing devices, and the formation of well-defined microstructures,^{1,4,5} but they present an excellent opportunity to study two-dimensional condensed organic solids at the microscopic level.

Chemisorption of the thiol main group to the surface results in long-range translational and orientational lattice structures. The investigation of the adsorption of functionalized thiols and disulfides on gold surfaces is becoming important for studies of phenomena at surfaces and interfaces, especially in the field of biomaterial science^{6,7} and biosensor technology.^{8–10} Alkyl thiols are known to form well-organized self-assembled monolayers (SAMs) on solid surfaces.¹¹ Such properties as packing density, molecular orientation, tilting angle, binding strength to substrate and stability alkyl thiols have been extensively studied for the last 15 years. The thermal stability for alkyl thiols has been studied and it has been shown that irreversible disordering of the alkyl chains occurs already at 80 °C. One way to improve the stability is to introduce lateral hydrogen bonds to increase

the intermolecular interactions. Several studies show lateral hydrogen bonding in thiols by including peptide bonds in the alkane chain.^{12,13}

A special kind of adsorbates with high potential is cysteine-containing peptides. These peptides can be linked to a gold surface through thiol chemistry and contain peptide bonds that induce formation of intermolecular hydrogen bonds, resulting in lateral stabilization. In this work we are studying arg-cysteamine molecules $\text{SH}(\text{CH}_2)_2\text{NHCOCH}(\text{NH}_2)_3\text{NHC}(\text{NH}_2)\text{NH}$, since arginine plays a specific role for G-protein recognition.¹⁴ The G-protein is important for the 7-helix transmembrane GPCR, which is a receptor for vision, odor sensing, and pain reception. The second and third intracellular loops and the C-terminal tail of the 2A GPCR are important sites for G-protein binding and interactions.^{15–17} It is of great interest to understand how G-proteins interact with the receptor and to find the minimum sequence of recognition. A peptide sequence with unique binding properties for G-protein would be invaluable, but even high selectivity for the G-protein would be excellent for drug screening. We have studied G-protein interaction of arginine-containing dipeptides by SPR.^{18,19} We also have ongoing studies of larger arginine-rich peptides with very promising results.

In this paper, a theoretical study of the ground state for the arg-cysteamine adsorbates is presented. The ground state energy of a monolayer self-assembled on Au(111) reveals a hexagonal structure of 2×2 . This is compared to the ordinary $\sqrt{3} \times \sqrt{3}$ structure reported for long-chained alkyl thiols. Theoretical calculations of phase transitions to tilted and twisted states for these adsorbates are also presented. Moreover, we studied the role of the hydrogen bonds. We found

^{a)}Electronic mail: almasa@ifm.liu.se, almas@tnp.krasn.ru

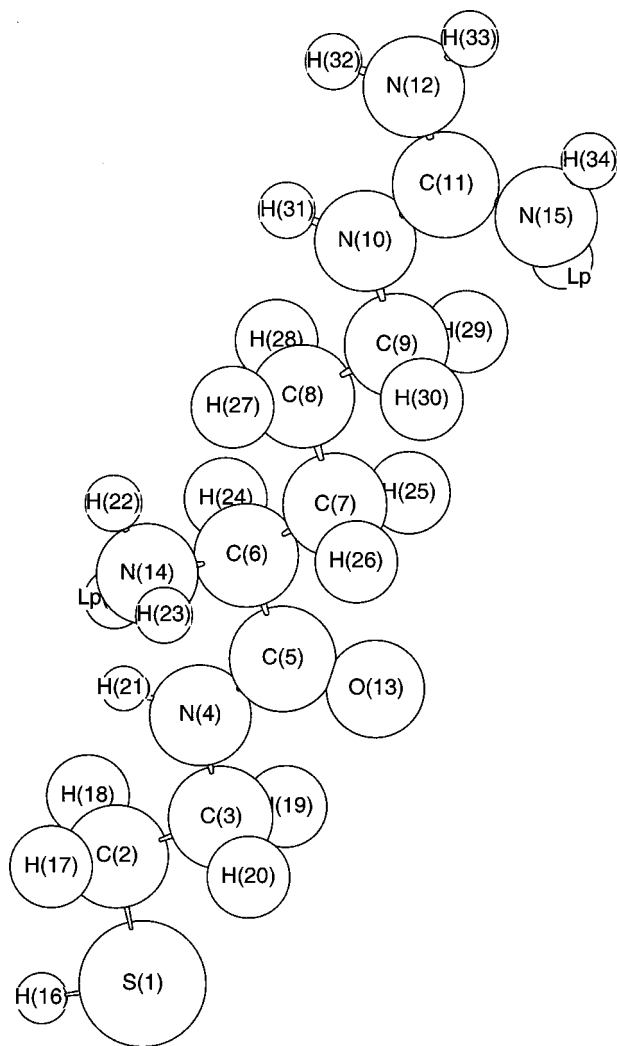


FIG. 1. View of an arg-cysteamine molecule. Spheres show atoms identified as, for example, S-1 as the type of atom and its number in the molecule, respectively. Two spheres denoted as Lp mean lone pairs which form additional dipole moments given in Table II.

that the hydrogen bonds in fact increase the temperature of phase transition by 40 K.

The ground state and phase transitions were studied theoretically mainly for self-assembled monolayers of alkanethiols deposited on the gold surface. The first approach is molecular dynamic simulations,^{20–25} which succeeded in establishing the ground state properties of the SAM and thermally equilibrium orientational states at fixed temperature. The second approach, developed in Refs. 28–30, is a symmetry analysis to study phase transitions in the mean field approximation. In the present paper we will use the last approach in application to the system of arg-cysteamines deposited on the Au(111) crystal surface.

II. MOLECULAR MODEL

The model adopted for the arg-cysteamine molecule shown in Fig. 1 consists of all 40 spherical atoms connected by rigid bond constraints. The molecule is chemically adsorbed on the crystal surface of gold (111) via the sulfur atom. Bond lengths were constrained to the

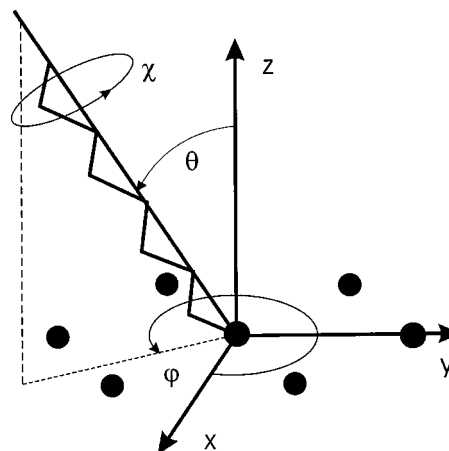


FIG. 2. Schematic drawing of three angles that specify position of arg-cysteamine molecule relative to the crystal surface (111) of gold (shown by black circles). θ is the tilt angle of the molecule, χ is the chain twist (rotation) angle, and φ defines the tilt direction along the surface plane.

following values:²³ $d_{CC}=1.54 \text{ \AA}$, $d_{CS}=1.82 \text{ \AA}$, $d_{CH}=1.04 \text{ \AA}$, $d_{CO}=1.23 \text{ \AA}$, $d_{CN}=1.45 \text{ \AA}$, $d_{HN}=1.02 \text{ \AA}$, and $d_{CN}=1.37 \text{ \AA}$ for the peptide linkage. Bond angles were set equal to the ideal valent ones. The molecular chain $\text{SH}(\text{CH}_2)_2\text{COH}(\text{NH}_2\text{CH}_2)_n$ has a zig-zag form as shown in Fig. 1, terminated by group NH_3 and all of them are represented by single interaction sites including hydrocarbons. The total length of the molecule is found to be 14 \AA .

We assume that the chain may freely rotate about the chain axis as a whole with the twisting angle as the dihedral angle between the plane composed of the normal to the gold surface, and the chain axis and plane defined by *trans* segments of the zig-zag molecular chain. Moreover, we assume that chain may rotate around the normal to the crystal surface in such a way that the sulfur does not take part in this rotation. This rotation is specified by two angles: the tilting angle θ and azimuthal projection φ (the precession angle of the long molecular axis about the surface normal to the gold crystal surface as shown in Fig. 2). All the atoms, including hydrogen, were represented by sites that interact with one another through potentials. The atom-atom potentials can be approximated in different ways. In Ref. 26 they are given as the van der Waals potential

$$V(r) = A e^{-Br} - \frac{C}{r^6} \quad (1)$$

with constants specified for each pair of identical atoms: C–C, N–N, O–O, H–H. The constants for unlike pairs of atoms can be calculated as $A_{ij} = \sqrt{A_i A_j}$, $C_{ij} = \sqrt{C_i C_j}$,²³ where i and j enumerate atoms. However this potential has a negative divergence for small distances. Hence, following Refs. 27–29, we take interactions between atoms of neighboring chains as the Lennard-Jones ones

$$U(R) = 4\epsilon \left[\left(\frac{\sigma}{R} \right)^{12} - \left(\frac{\sigma}{R} \right)^6 \right], \quad (2)$$

where parameters ϵ and σ were chosen by fitting the potential (2) to the Born-Meyer potential (1) in a way that both potentials have the same position and a depth of minimum.

TABLE I. Atom-atom Lennard-Jones parameters.

Atom pair	$\epsilon(K)$	$\sigma(\text{\AA})$
H-H	14.87	2.50
C-C	39.86	3.39
N-N	33.85	3.20
O-O	61.52	2.90
H-C	24.84	2.94
H-N	22.56	2.83
H-O	29.75	2.70
C-N	36.72	3.29
C-O	50.55	3.12
N-O	46.25	3.04
S-C	78.11	3.52
S-H	25.74	3.26

The calculated Lennard-Jones parameters ϵ_{ij} and σ_{ij} are listed in Table I.

The constants for the S-C and S-H couplings were taken from Ref. 31. In addition, the hydrogen bond interactions are considered as the Lennard-Jones potential (2) with parameters³² $\epsilon(K) = 226.4$ K, $\sigma = 2.168$ \AA, and the bond angles $\theta(\text{N-H}\cdots\text{O}) = 160^\circ \pm 5^\circ$ and $\theta(\text{H}\cdots\text{O}=\text{C}) = 150^\circ \pm 5^\circ$. These angles suggest the statistical significant tendency for hydrogen bonds to occur in the directions of the conventionally viewed oxygen sp^2 lone pairs.³³

Following Hautman and Klein,²¹ the interaction of atoms with gold substrate was modeled by the 12-3 potential,

$$V(z) = \frac{C_{12}}{(z-z_0)^{12}} - \frac{C_3}{(z-z_0)^3}. \quad (3)$$

In fact, this potential is sharply decreasing with distance z . Therefore, it is reasonable to include in (3) only interaction of the gold surface with the nearest atoms such as sulfur and the CH_2 group. The parameters of the potential (3) are the following.²¹ For the methylene group: $C_{12} = 2.8 \times 10^7$ K \cdot \AA¹², $C_3 = 17100$ K \cdot \AA³, $z_0 = 0.86$ \AA. For the sulfur: $C_{12} = 4.09 \times 10^7$ K \cdot \AA¹², $C_3 = 180600$ K \cdot \AA³, $z_0 = 0.27$ \AA.

Finally we took into account the dipole-dipole couplings of the dipole moments of different bonds formed by molecular groups. Moreover, we included the dipole moment of lone pair (lp) (Ref. 34) in the NH_2 and NH groups shown in Fig. 1,

$$W(\mathbf{R}_{ij}) = \sum_{\alpha,\beta} W_{ij}^{\alpha,\beta} d_i^\alpha d_j^\beta, \quad (4)$$

where

$$W_{ij}^{\alpha,\beta} = \frac{\delta_{\alpha,\beta}}{R_{ij}^3} - \frac{3R_{ij}^\alpha R_{ij}^\beta}{R_{ij}^5}, \quad (5)$$

and \mathbf{R}_{ij} is the vector between the dipole moments; the magnitude of a dipole moment is measured in the Debye units $D = 10^{-18}$ CGSE cm. Dipole moments were calculated with the help of the CS Gaussian Client package by Cambridge-Soft Corporation and are listed in Table II. The dipole moments are directed from the first atom to the second one in the bond. Numbers of atoms are presented in Fig. 1.

TABLE II. Dipole moments of molecular bonds.

Bond	Dipole moment (Debye)
S(1)-C(2)	1.2
H(21)-N(4)	0.5
C(5)-O(13)	2.3
H(22)-N(14)	0.76
H(23)-N(14)	0.76
Lp of N(14)	0.6
C(9)-N(10)	1.26
H(31)-N(10)	0.87
C(11)-N(10)	0.87
C(11)-N(12)	0.87
C(11)-N(15)	0.58
H(32)-N(12)	0.55
H(33)-N(12)	0.55
H(34)-N(15)	0.58
Lp of N(15)	0.6

By distances between atoms and bond angles one can find the coordinates of atoms in the local coordinate system with $\theta = 0$, $\varphi = 0$, and $\chi = 0$. The distances are listed in Table III. The bond angle for carbon groups is 109.5° and the bond angle for nitrogen groups is 107.3° .³⁴ We neglect slight distortions of these angles as the molecular groups are bonded in the arg-cysteamine molecule.

To find the coordinates defining the carbon and hydrogen atoms of the n -thiol chain in the coordinate system of the substrate it is necessary to use transformations of rotations determined by the Euler angles. This procedure is described in Ref. 28 and is not given here.

III. THE SYMMETRY OF THE GROUND STATE AND PHASE TRANSITIONS

In order to find possible phase transitions in the system of arg-cysteamine molecules self-assembled on the gold surface it is necessary to consider the symmetry of the system in the ground state. Then phase transitions can be classified as consequent spontaneous breakdown of this symmetry.³⁵

As a first step, we assumed there were two types of self assembly of the arg-cysteamine molecules on the gold surface (111), as shown in Fig. 3. The first type corresponds to the SH main groups of the arg-cysteamines, which form a $(\sqrt{3} \times \sqrt{3})R30^\circ$ lattice shown in Fig. 3 by black circles similar to the alkanethiol self-assembly.²⁸ The second type is the 2×2 lattice shown in Fig. 3 by gray circles. The gold atoms are shown by light circles. For each type of lattice the total energy of the self-assembly consisted of

TABLE III. Atom-atom distances.

Atom-atom	Distances (\AA)
C-S	1.82
C-C	1.54
C-N	1.45
C-H	1.09
C-O	1.23
N-H	1.02
Peptide linkage C-N	1.37

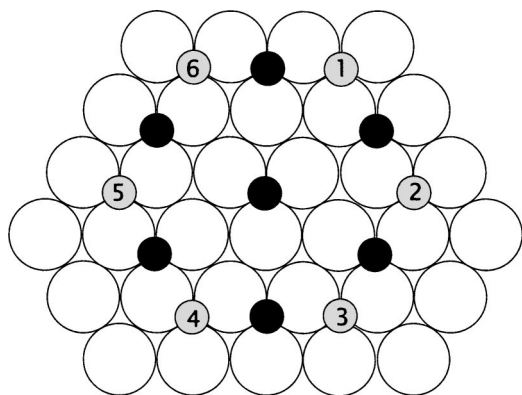


FIG. 3. Two patterns of self-assembly of the SH main groups on the gold crystal surface (111) shown by black circles [the $(\sqrt{3}\times\sqrt{3})R30^\circ$ lattice] and by gray circles (the 2×2 lattice). The gold atoms are shown by light circles.

$$E(\varphi, \theta, \chi) = N \sum_{j=1}^6 \sum_{nn_j} \left[U(|\mathbf{R}_n(\varphi, \theta, \chi) - \mathbf{R}_{n_j}(\varphi, \theta, \chi)|) + N \sum_n V(z_n(\varphi, \theta, \chi)) + E_d \right], \quad (6)$$

where index j runs over the nearest neighbors; indexes n and n_j run over atoms of the arg-cysteamine molecule, N is the number of the arg-cysteamines in the unit area and E_d is the total dipole energy of all dipole moments listed in Table II, computed by Ewald's method.^{30,36} A single dipole spaced apart from a metal experiences an interaction with its self-image, so a dipole-dipole part of the dipole energy consists of dipole-dipole, dipole-image, and image-image interactions. Equation (6) is the basic equation, a variation of which allows us to find the ground state of the arg-cysteamines adsorbed on the Au(111) crystal surface and symmetry of the system.

A variation of Eq. (6) relative to the angles gives us the following result. For the $(\sqrt{3}\times\sqrt{3})R30^\circ$ lattice we obtained $E_0 = 435.50 \text{ K}/\text{\AA}^2$ with $\varphi_0 = 41^\circ$, $\theta_0 = 1.7^\circ$, $\chi_0 = 2^\circ$, while for the 2×2 lattice we obtained $E_0 = 344.9 \text{ K}/\text{\AA}^2$ with $\varphi_0 = 84^\circ$, $\theta_0 = 4.7^\circ$, $\chi_0 = -41^\circ$. Therefore, the 2×2 structure is more stable relative to the $(\sqrt{3}\times\sqrt{3})R30^\circ$ lattice. Moreover, since the 2×2 lattice has the lower surface density in comparison with the $(\sqrt{3}\times\sqrt{3})R30^\circ$ lattice, the equilibrium angles fixing the arg-cysteamines relative to the crystal surface are larger in the former lattice.

Next, consider a symmetry of the system. First of all, the system is degenerated relative to rotations of the symmetry group C_6 because of the hexagonal symmetry of the crystal surface. Moreover, as was shown for the n -alkanethiols on

the crystal surface of gold (111) (Refs. 28, 29) in tilted phase, there is additional Z_2 symmetry with twofold degeneracy. The same $C_6\times Z_2$ symmetry is observed for the arg-cysteamines chemisorbed on the gold crystal surface (111). A minimization of the total energy results in the following equilibrium angles:

$$\begin{aligned} |1,n\rangle &= (\varphi_0 = 84^\circ + \pi n/3, \chi_0 = -41^\circ, \theta_0 = 4.7^\circ), \\ |2,n\rangle &= (\varphi_0 = -4^\circ + \pi n/3, \chi_0 = 41^\circ, \theta_0 = 4.7^\circ), \end{aligned} \quad (7)$$

where $n = 0, \dots, 5$. Therefore, the total symmetry of the system is $C_6\times Z_2$. A spontaneous symmetry breakdown of the C_6 symmetry gives rise to the tilted state, while the spontaneous symmetry breakdown of the Z_2 symmetry gives rise to the twisted state.²⁸

Let us consider at first the possibility of the phase transition to the tilted state. Six degenerated states in the ground state are specified by angles (7). Let us consider the central arg-cysteamine molecule and its six nearest neighbors at sites $j = 1, 2, \dots, 6$ shown in Fig. 3 by gray circles. The state of each molecule is given by the number $n_j = 0, \dots, 5$ in Eq. (7). Then the energy of the system mapped on to states (7) can be written as

$$\sum_{\langle i,j \rangle} \sum_{n_i, n_j} E(n_i, n_j), \quad (8)$$

where $\langle i,j \rangle$ means that we take into a consideration only the nearest-neighbor interaction.

If the molecules were linear chains we would have only three energies of interaction $E(n, n+m)$, $m = 0, 1, \dots, 5$ independent of the sites of the nearest neighbors j . However, because of the complicated structure of the arg-cysteamine molecule shown in Fig. 1 we obtain a higher number of the interaction constants $E(n_i, n_j)$ which depend on both the integers n_i, n_j and the positions of the molecules. Substituting the states (7) into (6) we have calculated the interaction constants listed in Table IV.

Note that because of the symmetry $J_j(n, n') = J_j(n+m, n'+m)$ we presented in this table only $J_j(1,1), J_j(1,2), \dots, J_j(1,6)$. Moreover, because of cyclic symmetry, for example, $J_j(7,2) = J_j(1,2)$.

Let us introduce occupation numbers $c_n = 0, 1$. Then each pair interaction (8) can be presented as a

$$E = \sum_j \sum_{nn'} J_j(n, n') c_n c_{n'}. \quad (9)$$

Similar to the mean-field theory of the Potts model³⁷ we introduce $x_n = \langle c_{jn} \rangle$, which are the fraction of the molecules that are in the state $n = 1, 2, \dots, 6$, subject to

TABLE IV. Interaction constants $J_j(n, n')$ in K.

n_j	1	2	3	4	5	6
$j=1$	-1733	-1231	436	-788	-810	-996
$j=2$	-810	-695	-536	-391	-750	-1186
$j=3$	-1336	-996	-750	-1224	1.6×10^7	-773
$j=4$	-1733	-1186	1.6×10^7	9685	-2555	-2118
$j=5$	-810	-773	-2555	-1961	-1611	-1231
$j=6$	-1336	-2117	-1611	-1374	436	-694

$$\sum_n x_n = 1. \quad (10)$$

Then, to the mean-field energy and entropy per molecule are

$$\begin{aligned} \frac{E}{N} &= \frac{1}{2} \sum_{j=1}^6 \sum_{nn'} J_j(n, n') x_n x_{n'}, \\ \frac{S}{N} &= -k \sum_n x_n \ln x_n, \end{aligned} \quad (11)$$

where the interaction constants $J_j(n, n')$ are listed in Table IV. Then the free energy per molecule is given by the expression

$$F = kT \sum_n x_n \ln x_n + \frac{1}{2} \sum_{n, n'} K(n, n') x_n x_{n'}, \quad (12)$$

where matrix $K(n, n') = \sum_j J_j(n, n')$ equals

$$K = \begin{pmatrix} -7757 & -6998 & 1.6 \times 10^7 & 3946 & 1.6 \times 10^7 & -6998 \\ -6998 & -7757 & -6998 & 1.6 \times 10^7 & 3946 & 1.6 \times 10^7 \\ 1.6 \times 10^7 & -6998 & -7757 & -6998 & 1.6 \times 10^7 & 3946 \\ 3946 & 1.6 \times 10^7 & -6998 & -7757 & -6998 & 1.6 \times 10^7 \\ 1.6 \times 10^7 & 3946 & 1.6 \times 10^7 & -6998 & -7757 & -6998 \\ -6998 & 1.6 \times 10^7 & 3946 & 1.6 \times 10^7 & -6998 & -7757 \end{pmatrix}. \quad (13)$$

On the basis of numerical values of matrix (13) it follows that the free energy (12) can be presented approximately as

$$F = kT \sum_n x_n \ln x_n - \frac{1}{2} K_1 x_n^2 - K_2 x_n x_{n+1}, \quad (14)$$

where $K_1 = 7757$ K, $K_2 = 6998$ K. The free energy is to be minimized relative to six-manifold variables x_n subject to (10) and $\sum_n x_n x_{n+2} = 0$, $\sum_n x_n x_{n+3} \approx 0$. The last equations follow from matrix elements (13). In contrast to the Potts model,³⁷ a nonlinear procedure to minimize this free energy is a hard task even numerically. However, it is obvious that the critical temperature of the phase transition is basically determined by matrix elements K_1, K_2 to be estimated as $T_c \sim (K_1 + K_2)/2 \ln 5 \approx 5000$ K by an analog with the Potts model.³⁷ Therefore, we can conclude that the self-assembled monolayer of the arg-cysteamine molecules is always in the tilted state with the 2×2 lattice structure.

Now, let us consider the possibility of the next phase transition related to spontaneous breakdown of the remaining Z_2 symmetry. The Z_2 symmetry allows us to crucially simplify a consideration by reducing the total energy of the system to the Ising model. Following the same procedure as developed in Refs. 28 and 30, we write the following expressions for the rotated atom's coordinates:

$$\mathbf{R}_s = \mathbf{R}(s\varphi_0, \theta_0, s\chi_0) = \mathbf{R}_0 + s\mathbf{R}_1, \quad s = \pm 1, \quad (15)$$

where \mathbf{R}_0 is directed along the x -axis (along the next-nearest neighbor) and \mathbf{R}_1 is perpendicular to \mathbf{R}_0 . Then the atom's coordinates of the j th arg-cysteamine molecule are specified as follows:

$$\mathbf{R}_{jn} = \mathbf{R}_j + \mathbf{R}_{0,n} + s_j \mathbf{R}_{1,n}, \quad (16)$$

where n specifies the n th atom of the molecule. Then the total energy is reduced to

$$E = E_0 - \frac{1}{2} \sum_{ij} J_{ij}(\theta_0, \varphi_0, \chi_0) s_i s_j, \quad (17)$$

where $s_i = \pm 1$, and

$$J_{ij} = \frac{1}{4} \sum_{s, s'} s s' (U_{s, s'}^{ij} + W_{s, s'}^{ij}), \quad (18)$$

$$U_{s, s'}^{ij} = \frac{1}{2} \sum_{nn'} U_{nn'}(\mathbf{R}_{ij} + \mathbf{R}_{0,n} - \mathbf{R}_{0,n'} + s\mathbf{R}_{1,n} - s'\mathbf{R}_{1,n'}), \quad (19)$$

$$\begin{aligned} W_{s, s'}^{ij} &= \sum_p W(\mathbf{R}_{ij} + (s - s')\mathbf{R}_{1,p}) \\ &+ \frac{1}{2} W(\mathbf{R}_{ij} + \mathbf{Z}_p + (s - s')\mathbf{R}_{1,p}), \end{aligned} \quad (20)$$

where the vector \mathbf{Z}_p runs over image dipoles. If restricting by the nearest neighbors, numerical evaluation of formulas (18)–(20) results in

$$J_1 = -61.3K, \quad J_2 = 148.3K, \quad J_3 = 40.7K. \quad (21)$$

As shown in Fig. 4 we have six nearest neighbors. However, three others coincide with (21). While the alkanethiols have the mirror plane of symmetry which gives rise to two exchange integrals,^{28,29} in the present case there is no such symmetry.

The phase transition temperature of the 2D Ising model on the triangular lattice is found exactly³⁸

$$\xi_1 \xi_2 + \xi_2 \xi_3 + \xi_1 \xi_3 = 1, \quad (22)$$

where $\xi_i = \exp(-\beta_c J_i)$, $\beta = 1/kT$. However, for the case described in (21), Eq. (22) has no solution. Therefore we have to return to model (17) in which summation runs over all sites because of dipole–dipole interactions (20). Then we can evaluate the temperature of the phase transition in the mean field approximation to obtain $kT_c = J(0) = \sum_j J_{ij}$. Performing the elementary but tedious procedure of summation of inter-

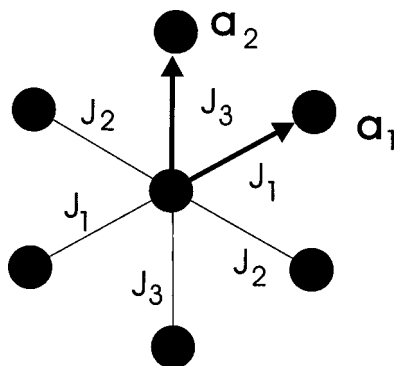


FIG. 4. Exchange integrals between the arg-cysteamines shown by the main atoms S (black circles). $\mathbf{a}_1, \mathbf{a}_2$ are unit vectors forming an elementary unit cell.

actions (19) and (20) with account of Tables I–III and substituting the result into Eq. (18) we obtained numerically $kT_{c2} \approx 340$ K. The summation over the dipole–dipole interactions (20) was performed using the Ewald procedure.³⁰ In order to find the role of the hydrogen bond interactions between the arg-cysteamine molecules we resumed all calculations, switching off these interactions. We found in this case $kT'_{c2} \approx 300$ K. Thus, indeed, the hydrogen bonds stabilize the SAM on the gold surface.

IV. DISCUSSION AND CONCLUSIONS

Calculation of the ground state energy of the system shows that the less dense 2×2 lattice is more favorable than the more dense $(\sqrt{3} \times \sqrt{3})R30^\circ$ lattice. Because of the C_6 symmetry of crystal surface Au(111) the self-assembled system of the arg-cysteamine molecules also has the same symmetry. Moreover, we established the symmetry Z_2 of the ground state of the system of arg-cysteamine molecules. As a result the total symmetry of the system is $C_6 \times Z_2$. In the mean field approximation we considered phase transitions which consequently spontaneously break this symmetry. We found that the critical temperature of the phase transition to the tilted state related to the breakdown of the C_6 symmetry $T_{c1} \approx 5000$ K is extremely high. Therefore, the self-assembled monolayer of the arg-cysteamine molecules is always in the tilted state with the tilting angle around 5° . This result agrees with estimations performed for the n -alkanethiols self-assembled on the Au(111) crystal surface.²⁸

The second phase transition takes place at room temperature $T_{c2} = 340$ K and leads to spontaneous twisting of the arg-cysteamine molecules related to the breakdown of the Z_2 symmetry. The value of the critical temperature qualitatively also agrees with the results obtained for the n -alkanethiols for $n = 12$.²⁸ However there are important differences between the alkanethiols and the arg-cysteamines self-assembled on the Au(111) crystal surface. The arg-cysteamine molecule shown in Fig. 1 is more bulky to compared to the alkanethiol molecule. As a result the arg-cysteamines are packing as the 2×2 lattice while the alkanethiols form the more dense $(\sqrt{3} \times \sqrt{3})R30^\circ$ lattice. Correspondingly the equilibrium angles (7) are strongly different

from the those of the alkanethiols. Therefore the exchange integrals (21), which define the temperature of the second phase transition to the twisted state, are also different in comparison to those for the alkanethiols self-assembled on the Au(111) crystal surface.

Both phase transitions were calculated with account of only discrete states of corresponding symmetry $C_6 \times Z_2$. However each molecule arg-cysteamine is oscillating around equilibrium positions. These vibrations form phonon modes in the self assembly contributed by bulk phonon modes of the gold crystal. In turn, these modes contribute to the entropy term of the free energy to decrease temperatures of phase transitions. So it is necessary to consider the critical temperatures found in this work as upper estimations. Moreover the calculated temperature of the phase transition T_{c2} to the twisted state has an accuracy in the same extend as the van der Waals potential interactions (1) with empirical choice of the constants by formulas given below (1). As was shown in Ref. 28 the value of critical temperature is rather sensitive to choice of the atom–atom interaction parameters. Hence we can conclude that the second phase transition to the twisted state takes place nearby room temperature while the phase transition to the tilted phase is extremely high.

ACKNOWLEDGMENT

This work was supported by a grant from The Royal Swedish Academy of Sciences (KVA).

- ¹J. D. Swalen, D. L. Allara, J. D. Andrade *et al.*, *Langmuir* **3**, 932 (1987).
- ²L. H. Dubois and R. G. Nuzzo, *Annu. Rev. Phys. Chem.* **43**, 437 (1992).
- ³R. G. Nuzzo, F. A. Fusco, and D. L. Allara, *J. Am. Chem. Soc.* **109**, 2358 (1987).
- ⁴P. E. Laibinis and G. M. Whitesides, *J. Am. Chem. Soc.* **114**, 9022 (1992).
- ⁵A. Kumar, H. A. Biebuyck, and G. M. Whitesides, *Langmuir* **10**, 1498 (1994).
- ⁶S. G. Zhang, L. Yan, M. Altman, M. Lassle, H. Nugent, F. Frankel, D. A. Lauffenburger, G. M. Whitesides, and A. Rich, *Biomaterials* **20**, 1213 (1999).
- ⁷L. P. Tang, L. Liu, and H. B. Elwing, *J. Biomed. Mater. Res.* **41**, 333 (1998).
- ⁸R. D. Vaughan, C. K. O'Sullivan, and G. G. Guilbault, *Fresenius' J. Anal. Chem.* **364**, 54 (1999).
- ⁹C. Cotton, A. Glidle, G. Beamson, and J. M. Cooper, *Langmuir* **14**, 5139 (1998).
- ¹⁰J. Rickert, T. Weiss, W. Kraas, G. Jung, and W. Gopel, *Biosens. Bioelectron.* **11**, 591 (1996).
- ¹¹A. Ullman, *Chem. Rev.* **96**, 1533 (1996).
- ¹²S. W. Tam-Chang, H. A. Biebuyck, G. M. Whitesides, N. Jeon, and R. G. Nuzzo, *Langmuir* **11**, 4371 (1995).
- ¹³R. C. Sabapathy, S. Bhattacharyya, M. C. Leavy, W. E. Cleland, and C. L. Hussey, *Langmuir* **14**, 124 (1998).
- ¹⁴S. M. Wade, M. K. Scribner, H. M. Dalman, J. M. Taylor, and R. R. Neubig, *Mol. Pharmacol.* **50**, 351 (1996).
- ¹⁵J. M. Taylor, G. C. Jacob-Mosier, R. G. Lawton, A. E. Remmers, and R. R. Neubig, *J. Biol. Chem.* **269**, 27618 (1994).
- ¹⁶S. M. Wade, H. M. Dalman, S. Z. Yang, and R. R. Neubig, *Mol. Pharmacol.* **45**, 1191 (1994).
- ¹⁷H. M. Dalman and R. R. Neubig, *J. Biol. Chem.* **266**, 11025 (1991).
- ¹⁸K. Uvdal and T. Vikinge, *Langmuir* **17**, 2008 (2001).
- ¹⁹R. M. Petoral Jr. and K. Uvdal, *Colloids Surf., B* **25**, 335 (2002).
- ²⁰C. M. Knobler and R. C. Desai, *Annu. Rev. Phys. Chem.* **43**, 207 (1992).
- ²¹J. Hautman and M. L. Klein, *J. Chem. Phys.* **91**, 4994 (1989).
- ²²J. Hautman and M. L. Klein, *J. Chem. Phys.* **93**, 7483 (1990).
- ²³W. Mar and M. L. Klein, *Langmuir* **10**, 188 (1994).
- ²⁴S. Shin, N. Collazo, and S. A. Rice, *J. Chem. Phys.* **98**, 3469 (1993).

- ²⁵M. A. Moller, D. J. Tildesley, K. S. Kim, and N. Quirke, *J. Chem. Phys.* **94**, 8390 (1991).
- ²⁶F. L. Hershfeld and K. Mirsky, *Acta Crystallogr., Sect. A: Cryst. Phys., Diffraction, Theor. Gen. Crystallogr.* **35**, 366 (1979).
- ²⁷A. Zangwill, *Physics at Surfaces* (Cambridge University Press, New York, 1988), Chap. 8.
- ²⁸A. F. Sadreev and Yu. V. Sukhinin, *Phys. Rev. B* **54**, 17966 (1996).
- ²⁹A. F. Sadreev and Yu. N. Sukhinin, *J. Chem. Phys.* **107**, 2643 (1997).
- ³⁰Yu. V. Sukhinin, *JETP* **87**, 115 (1998).
- ³¹W. L. Jorgensen, *J. Phys. Chem.* **90**, 6379 (1986).
- ³²Y. K. Kang, *J. Phys. Chem. B* **104**, 8321 (2000).
- ³³R. Taylor, O. Kennard, and W. J. Versichel, *J. Am. Chem. Soc.* **105**, 5761 (1983).
- ³⁴R. Chang, *Physical Chemistry for the Chemical and Biological Sciences* (University Science Books, Sausalito, 2000), Chap. 15.
- ³⁵L. D. Landau and E. M. Lifzhits, *Statistical Physics* (Pergamon, Oxford, 1980).
- ³⁶J. M. Ziman, *Principles of the Theory of Solids*, 2nd ed. (Cambridge University Press, Cambridge, 1972).
- ³⁷F. Y. Wu, *Rev. Mod. Phys.* **54**, 235 (1982).
- ³⁸R. J. Baxter, *Exactly Solved Models in Statistical Mechanics* (Academic, New York, 1982), Chap. 11.